EMBS 2003 Student Paper Finalists

Dynamic Time Warping in the Analysis of Event-Related Potentials

Computing Reliable ERP Templates from Dyslexic Children

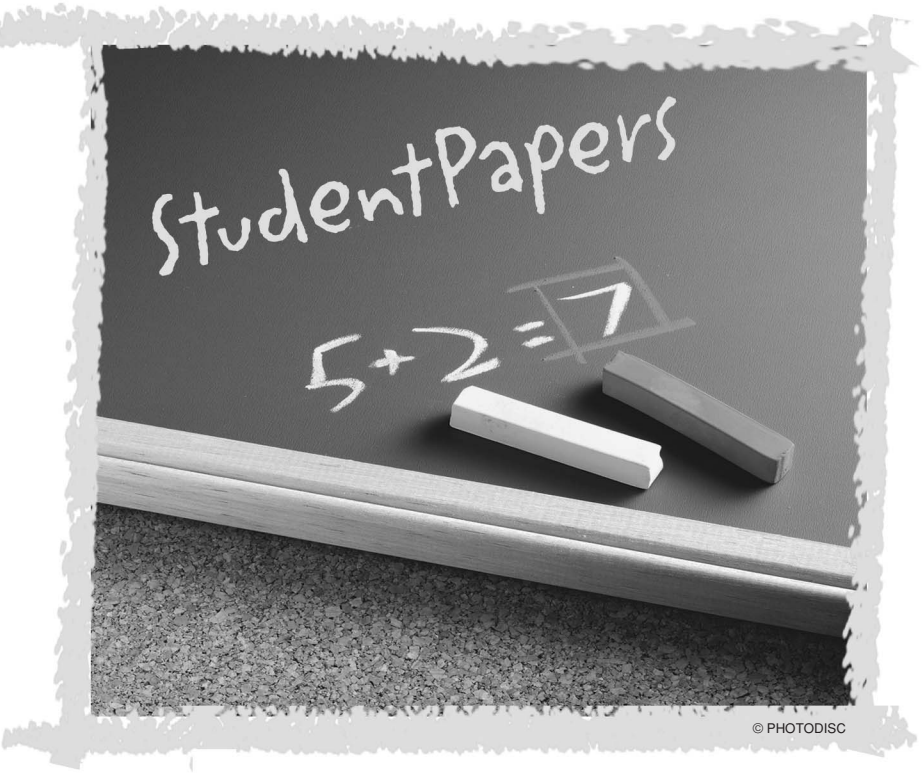

BY SILVIA CASAROTTO, ANNA M. BIANCHI, SERGIO CERUTTI, AND GIUSEPPE A. CHIARENZA

The aim of this article is to compute reliable templates of event-related potentials (ERPs) for homogeneous groups of subjects and to automatically quantify the morphological characteristics of the ERPs. We developed a method based on dynamic time warping (DTW). The method was applied to ERPs recorded from normal and dyslexic children during two reading tasks. We found that characteristic latency and amplitude changes of ERP components are due to task and pathology. Our results support the idea that dyslexia involves different and complex cerebral functions aside from the language system. This mathematical approach provides reproducible analysis criteria that are crucial for the reliability of ERP analysis.

Introduction

ERPs recorded during the execution of specific cognitive tasks are useful for studying higher-order cerebral functions. This approach is worthwhile because it allows the evaluation of brain behavior in vivo with high temporal resolution; furthermore, it is noninvasive, easy to apply, and low in cost. These characteristics make it particularly suitable in children studies. We recorded ERPs in normal children and in children with developmental dyslexia to study the neurophysiological bases of reading processes. Developmental dyslexia is a neuropsychological disorder that involves reading abilities and coexists with average intelligence, adequate

 0739-5175/05/$20.00©2005IEEE

education, and normal sensory acuity. There is not full agreement among researchers about the structural and functional origins of dyslexia, and several models have been proposed [1]–[4]; the most recent theories hypothesize a genetic disruption of the cerebral structure that would affect phonological awareness and visual/auditory perception [5], [6]. This disorder is sometimes reversible when specific rehabilitative therapies are performed on young children [7]. Therefore, it is important to deeply investigate the reading processes in order to diagnose dyslexia as early as possible and to work out efficacious and tailored treatments.

The analysis of ERPs is based on the quantification of their morphological characteristics, primarily the latency and amplitude of the most relevant components. Group analysis usually stems from the computation of grand averages of ERPs on homogeneous subjects.

Cognitive potentials are characterized by a great intra- and interindividual variability, and their morphology is deeply influenced by age and pathology. The components with long latency significantly vary with scalp site and stimulation paradigm [8].

The marked variability of cognitive potentials recorded in children has important consequences for the analysis and interpretation of their morphological characteristics. First, the components resulting from intersubject grand averaging appear smoothed because of latency variability; therefore peaks detection loses precision. Furthermore, the identification of the relevant components must be manually performed by skilled researchers after long and complex training. Due to the variable characteristics of these potentials, the analysis approach is often slightly modified as observations and experience increase. For these reasons, the quantification of ERPs' morphology is time-consuming and greatly affected by the subjective judgment of the experimenter.

This work describes a nonlinear alignment method based on the DTW technique for computing reliable ERP templates for homogeneous groups of subjects and for automating the quantification of ERPs' morphology. The results obtained from comparing reading-related potentials recorded from both normal and dyslexic children are also reported.

Method

DTW is a nonlinear alignment algorithm that reduces the temporal differences between morphologically similar signals through local compressions and extensions of their temporal axes [9]–[10]. The analytic procedure followed by the method consists in two different steps performed on paired signals. The first step is the identification of the best correspondence between the samples of the signals according to certain criteria of similarity. The second step consists of building up a new signal by condensing the morphological characteristics of those signals from which it was computed.

Given the two signals:

$$\mathbf{x} = \{x(i)\ 1 \le i \le I\}$$

$$\mathbf{y} = \{y(j)\ 1 \le j \le J\}$$

with the same sampling rate, it is possible to graphically depict a temporal correspondence between their samples in a Cartesian plot, as shown in Figure 1. The line linking the associated samples is called the warping function (WF):

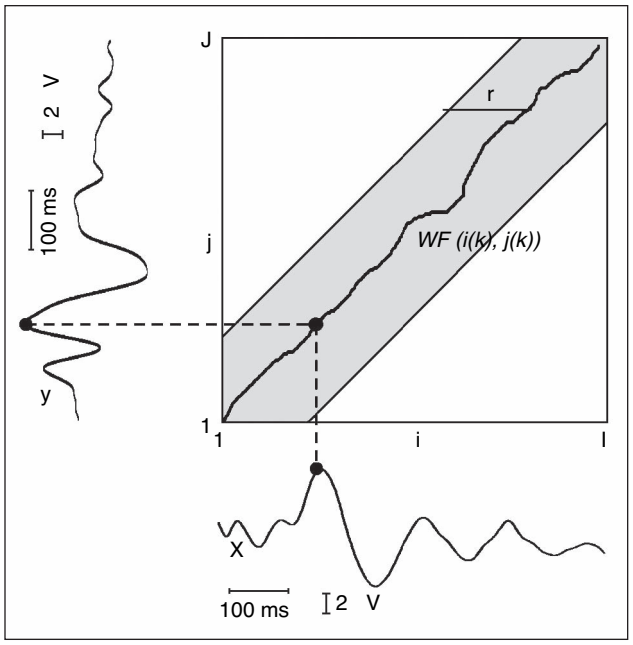

Fig. 1. An example of a warping function $(WF(i(k), j(k)))$ computed on the sampled signals $x(i)$ and $y(j)$.

$$\mathbf{WF} = \{\boldsymbol{WF(k)} = \big(\boldsymbol{i(k)}, j(k)\big)\ 1 \le k \le K\}$$

$$\text{with } \max(I, J) \le K < I + J - 1.$$

The WF has to respect the boundary limitations: $WF(1) = (1, 1)$ and $WF(K) = (I, J)$. This means that the first and the last samples of the signals $x(i)$ and $y(j)$ have to be associated together. In this way, all the signals samples are considered in the alignment. Furthermore, the WF has to be continuous and monotonic, not decreasing. As a consequence, the association between the samples of the signals is univocal without skips of samples. In order to prevent excessive adjustment of the time axes during alignment, the WF has to be confined in the region around the main diagonal defined by the following relation:

$$|i(k) - j(k)| \le r.$$

This constraint prevents that two samples of the signals farther than r samples are associated together. Due to the noise usually superimposed on the signals, it is advisable to avoid the WF following the noise more than the signal. With this intent, the following slope constraint condition was imposed:

$$p = n/m$$

where n represents the number of diagonal segments and m the number of horizontal or vertical segments that the WF can consecutively contain. This constraint prevents, after m consecutive horizontal or vertical segments, the WF stepping further in the same direction without making at least n consecutive diagonal segments.

The latency variability of cognitive ERPs produces a marked smoothing of their components when averaging across subjects is applied.

In case of no distortion, the WF is equal to the main diagonal. The only allowed moves of the WF are: horizontal (compression axis *j*), vertical (compression axis *i*), and diagonal (no compression axes *i* and *j*).

In order to compute the WF, a measure of the morphological distance between the samples of the signals was defined. This measure was called *dissimilarity function* and was described by the following equation:

$$d(k) = \left|x_n\big(i(k)\big) - y_n\big(j(k)\big)\right| + \left|x'_n\big(i(k)\big) - y'_n\big(j(k)\big)\right|$$

where the apex $'$ indicates first derivative and n indicates normalization between 0 and 1. This function was computed at every point of the warping plane, satisfying the previously imposed constraints. Wishing to align the signals according to their morphological similarity, the association between their samples is obtained by minimizing the following figure of merit:

$$D(\mathbf{x}, \mathbf{y}) = \frac{\sum_{k=1}^{K} d\,(k)\, s\,(k)}{\sum_{k=1}^{K} s\,(k)}$$

where the weights *s(k)* determine if the compression or extension of the temporal axis of one signal has to be privileged in comparison with the other. In the present work, we assumed that all the signals conveyed the same information; therefore a symmetric alignment was performed by computing the weights *s(k)* as indicated below:

$$s(k) = \big(i(k) - i(k-1)\big) + \big(j(k) - j(k-1)\big)$$

with $\sum_{k=1}^{K} s\,(k) = I + J$.

Applying dynamic programming principles, a matrix $\underset{(I,J)}{\mathbf{G}} = [g(k)] = [g(i(k),\ j(k))]$ was computed as follows:

$$g(k) = \min_{k-1}\big[g(k-1) + d(k)s(k)\big]$$

with the initial condition:

$$g\big(W(1)\big) = g(1, 1) = d(1, 1)s(1),$$

The generic element $g(k)$ measures the minimum cost to reach the point $(i(k), j(k))$ from $(1, 1)$. The WF representing the best alignment between the whole signals corresponds to the path in matrix $\mathbf{G}$ with the minimum cost reaching the point (I, J) from the point $(1, 1)$.

At this stage, a new waveform (template) is computed by averaging the original signals according to the WF. This new waveform condenses the morphological characteristics of the signals $x(i)$ and $y(j)$ without being distorted by the latency differences between their components. We obtained the template by applying the double-mean technique consisting of three steps. The first step produces a vector $\mathbf{r}$, that appears as follows:

$$\mathbf{r} = \Big[\ldots\ x\big(i(k)\big)\ \ y\big(j(k)\big)\ \ x\big(i(k+1)\big)\ \ y\big(j(k+1)\big)\ \ \ldots\Big].$$

The pair $[x(i(k))\quad y(j(k))]$ is repeated two times when the segment between $WF(k-1)$ and $WF(k)$ is diagonal.

The second step consists in the computation of a first average $m(a)$ according to the following:

$$m(a) = \frac{r(b) + r(b+1)}{2}.$$

The last step allows the computation of the template as an average of the signal $m(a)$:

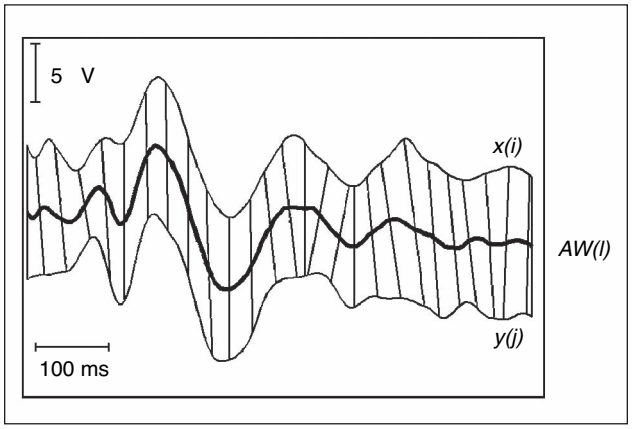

Fig. 2. The alignment of the sampled signals $x(i)$ and $y(j)$. The segments between the traces represent the temporal correspondence between morphologically similar samples of the two signals. The thick line represents the template computed with the double-mean technique after aligning $x(i)$ and $y(j)$.

$$AW(l) = \frac{m(a) + m(a+1)}{2}.$$

Figure 2 shows the temporal correspondence between two signals, $x(i)$ and $y(j)$, after alignment and the template resulting from the double-mean technique.

The computation of the template on more than two signals is realized by iteratively applying the method described above to paired signals following a binary tree structure, as shown in Figure 3.

After the computation of a template on a set of signals, the alignment of the template with each of the original signals produces a temporal correspondence between the samples of the template and the signals. As a consequence, the temporal location of physiologically relevant components detected on the template is automatically identified on the original signals, thus quantifying averaged ERPs' morphology.

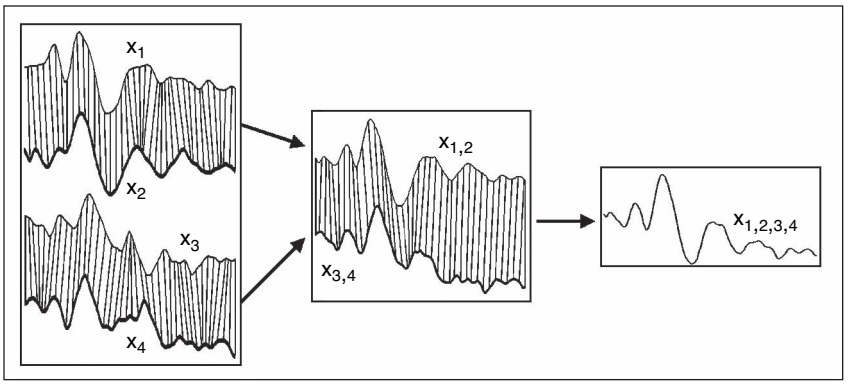

Fig. 3. The computation of a template on four signals (x_1, x_2, x_3, x_4). The thin segments represent the temporal correspondence between the samples of the signals. The method is applied to x_1, x_2, thus obtaining $x_{1,2}$, and to x_3, x_4, thus obtaining $x_{3,4}$. Then, the method is applied to $x_{1,2}, x_{3,4}$, thus obtaining the template $x_{1,2,3,4}$.

Experimental Protocol

Subjects

Thirty-two normal children (nine females and 23 males) ranging in age from 8.17 to 10.75 years (mean age 9.56 ± 0.67 years) and 16 children with developmental dyslexia (three females and 13 males) ranging in age from 8 to 10.58 years (mean age 9.05 ± 0.84 years) participated in the experiment. The children with developmental dyslexia were diagnosed according to DSM IV-R criteria [11], and the discrepancy between chronological age and reading age was obtained using the Direct Test of Reading and Spelling (TDLS), the Italian adaptation of the Boder test [12], [13]. All children were informed of the experimental procedure, and written consent was obtained from parents and children. The entire experimental protocol was approved by the hospital's ethical committee.

Experimental Setting

The stimuli consisted of the central presentation of 21 Italian alphabetic capital and small letters produced by a vacuum fluorescent display (brilliance: 175 fLumen). Each stimulus was 8 or 6 mm high for capital and small letters, respectively, and 3.5 mm wide, and its persistence on the screen was 25 ms. A minimum of four sets of stimuli were presented in the same random order for all subjects. When cooperation was poor, in the case of some dyslexic children, it was necessary to increase the number of stimuli. The distance between the examined subject and the display was 70 cm, and the angle of reading was 0.29.

Reading-related potentials were recorded during two conditions. The first condition, letter presentation (LPR), was passive: subjects passively watched letters without making any effort to read or articulate them silently. The second condition, letter recognition (LRE), was active: subjects read aloud the letters randomly appearing on the screen after the technician pressed a button. Single, isolated letters were used instead of words to avoid semantic inferences from context that might influence the reading processes of dyslexic children. Subjects sat in a dimly illuminated, electrically and acoustically shielded room.

EEG Recording

EEG was recorded using Ag-AgCl electrodes from Fz, Cz, Pz, Oz, $C4'$, $C3'$, $T4$, $T3$, $P4$, $P3$, referred to linked mastoids. Resistance was less than 10 kΩ. The EOG was bipolarly recorded using two electrodes diagonally placed above and below the right eye. Electroencephalogram (EEG) and electrooculogram (EOG) recordings were bandpass filtered between 0.02–30 Hz. Lip movements were bipolarly recorded by two electrodes placed on the superior and inferior orbicularis oris muscles; this electromyograph (EMG) signal was bandpass filtered between 160–3,000 Hz. Electrocardiogram (ECG) and pneumogram were also recorded, and bandpass was filtered between 0.005–3,000 Hz. A microphone was used to record the subjects' voices. The EEG and EOG signals were sampled at 250 Hz with 4 s analysis time, 2 s pre- and 2 s poststimulus.

Analysis Protocol

Before averaging, the trials affected by artifacts generated by nonocular sources of noise (gross body movements, muscular activity, etc.) were rejected by visual inspection. Artifacts from ocular movements and blinks were reduced by applying principal component analysis as described in [14], thus improving the signal-to-noise ratio (SNR) of averaged ERPs.

All ERPs were divided into four sets: two for the two tasks in the control group and two for the two tasks in the group with dyslexia. Alignment was separately performed on each set of potentials: four templates were obtained by iteratively applying DTW to pairs of signals according to a binary tree. Since each set contained a number of signals equal to a power of two, the binary tree was well balanced and all the original signals equally contributed to the template. The method was not applied to the entire ERP recording window but to the signal recorded in the first 700 ms poststimulus time. This restriction allowed reduction of the computing time and was large enough to contain most of the ERP components of interest. The parameters associated to the boundaries of the WF were empirically set to the following values: $r = 8$ samples (corresponding to 32 ms) and $p = 1$.

A skilled technician analyzed the templates to detect the most relevant ERP components. The temporal location of these components on averaged ERPs was automatically computed by aligning each original ERP with the corresponding template.

The templates were superimposed on traditionally computed grand averages to point out the advantages of the method in reducing jitter effect due to the potentials' latency variability. A two-sided t-test analysis was performed to evaluate the dissimilarities in latency and amplitude of the relevant ERP components between the two groups of children during the two reading tasks (we considered significant the differences with $p < 0.025$). The automatically identified ERP components were compared to the manual measurements in order to quantify the efficacy of the method.

Results

Comparison Between Grand Averages and Templates

Figure 4 shows the superimposition of grand averages (thick lines) and templates (thin lines) computed on the ERPs recorded from *C3′* and *P3* channels in 32 normal children during the letter presentation task. The latency variability of cognitive ERPs produces a marked smoothing of their components when averaging across subjects is applied. As a consequence, certain waves can be hardly detected on the traces because their amplitude is clearly reduced (see Figure 4). The deformation of the temporal axes performed by DTW allows the corresponding peaks and troughs to align before interindividual averaging. Therefore, the template's morphology is sharper than that of the grand averages, and the ERP components are easier to identify.

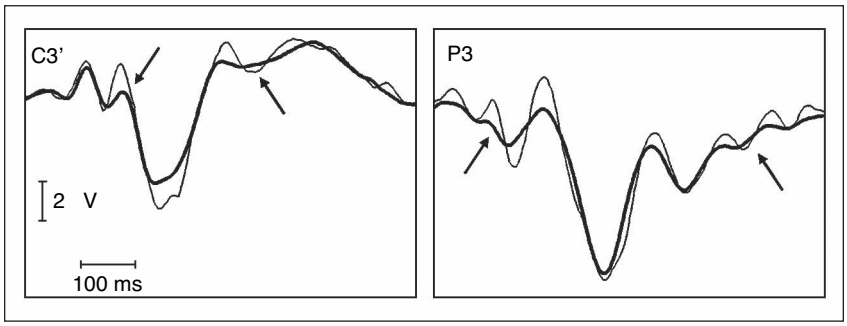

Fig. 4. A superimposition of grand averages (thick lines) and templates (thin lines) computed on the ERPs recorded from *C3′* and *P3* channels in 32 normal children during the letter presentation task. The most evident differences between grand averages and templates are marked.

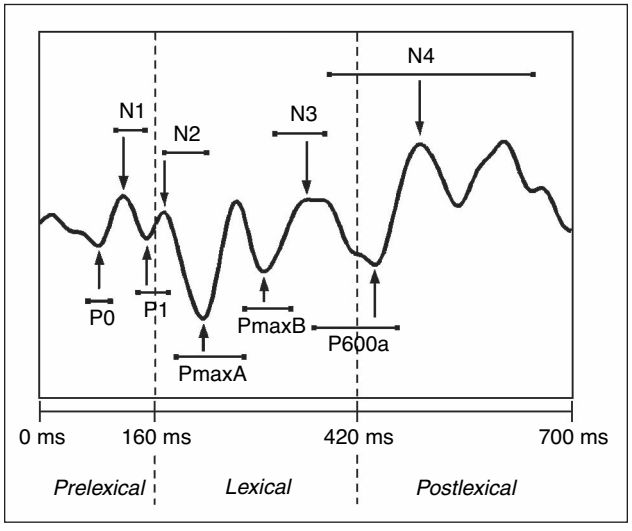

Fig. 5. The chronology of ERP components during reading aloud recorded from *C4* in a normal subject.

Analysis of Reading-Related Potentials in Normal and Dyslexic Children

The exact functional meaning of reading-related potentials is not precisely known. On the basis of the EMG activity of the lips, however, it is possible to divide their components into three periods based on their latency range [15], [16]. Figure 5 shows an averaged ERP and the physiologically relevant peaks and troughs that can be identified on its trace. The components with latency less than 160 ms (P0, N1, P1) belong to the prelexical period; they are associated with sensory processing of stimuli. P1 is particularly evident in *Oz*, because it denotes the activation of the primary visual cortex in correspondence to stimuli presentation. The components with latency in the range 160–420 ms (N2, PmaxA, PmaxB, N3) belong to the lexical period; they are mainly concerned with stimulus categorization. The components appearing after 420 ms (P600a, N4, P600b) belong to the postlexical period; they presumably reflect long-term semantic memory and feedback processes.

We compared the latency and amplitude of the most relevant ERP components between the two reading tasks in each group of children and between the two groups of children for each reading task. Figures 6–9 show the superimposition of different ERP templates in all the recording sites. Each figure is associated with two tables: the significant latency differences are contained in Tables 1–4(a) and the significant amplitude differences in Tables 1–4(b).

Figure 6 shows the superimposition of the templates computed for the ERPs recorded in normal children during the letter presentation (thin lines) and the letter recognition (thick lines) tasks. The latency of prelexical and lexical components (N1, PmaxB) increased, passing from LPR to LRE, while that of the postlexical components decreased (P600b). These latency differences were statistically significant in the parietal regions. The amplitude of the ERP components in the LRE task is always significantly greater than in the LPR task; this is evident in the lexical and postlexical periods and almost on all recorded cerebral regions. Significant differences between the two templates are marked by arrows.

The templates obtained from the two reading tasks by the children with dyslexia are depicted in Figure 7. The latency of N1 in frontal and central regions and of N3 in occipital and left-parietal regions significantly decreased, passing from LPR to LRE. The amplitude of the components recorded in the LRE task is always significantly greater than in the LPR task. No significant amplitude differences were found in the lateral-parietal regions.

The comparison between the ERP templates of normal children (thin lines) and of children with dyslexia (thick lines)

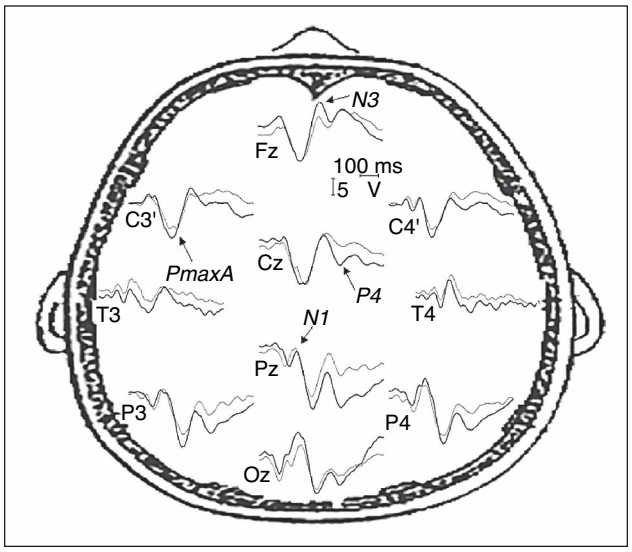

Fig. 6. A superimposition of the ERP templates obtained from the control group during the LPR (thin lines) and LRE (thick lines) tasks. Arrows mark significant differences of latency and amplitude between the two potentials ($p < 0.025$).

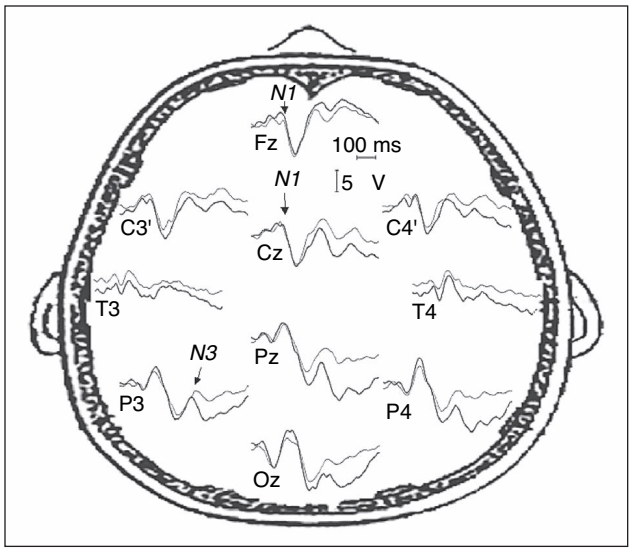

Fig. 7. A superimposition of the ERP templates obtained from the group with dyslexia during the LPR (thin lines) and LRE (thick lines) tasks. Arrows mark significant differences of latency and amplitude between the two potentials ($p < 0.025$).

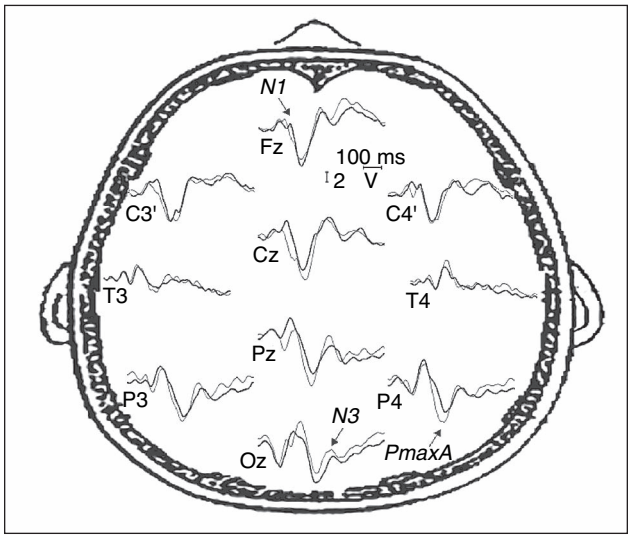

Fig. 8. A superimposition of the ERP templates obtained during the LPR task from the control group (thin lines) and the children with dyslexia (thick lines). Arrows mark significant differences of latency and amplitude between the two potentials ($p < 0.025$).

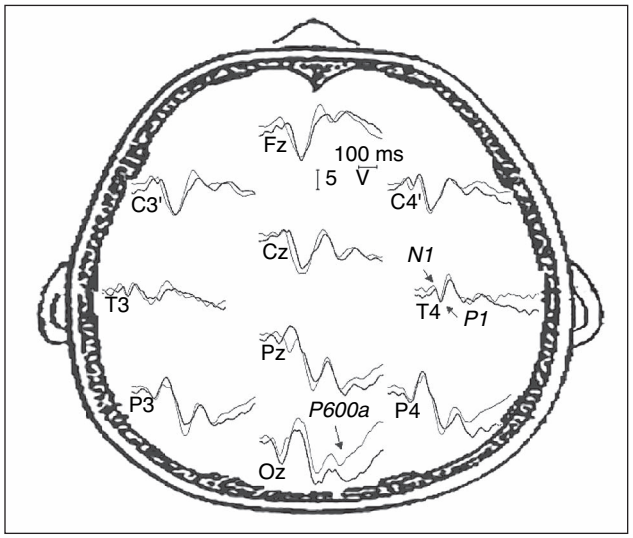

Fig. 9. A superimposition of the ERP templates obtained during the LRE task from the control group (thin lines) and the children with dyslexia (thick lines). Arrows mark significant differences of latency and amplitude between the two potentials ($p < 0.025$).

during the letter presentation task is plotted in Figure 8. The latency of most of the components is significantly greater in dyslexic children in comparison with controls. No significant differences were noticed in the temporal regions. Considering the amplitude, only N2 in *Cz* is significantly higher in dyslexics compared to controls.

For the letter recognition task, the templates computed from the two groups of children are shown in Figure 9. In the ERP components recorded from dyslexic children in the temporal and occipital regions, there was a general increase of latency in comparison with normal children. The significant amplitude differences were located in the left hemisphere (channels *C*3′ and *P*3) and consisted of an amplitude reduction of N3 and an amplitude increase of N2.

Quantification of the Method Performances

Considering the ERPs recorded from all the subjects in the two conditions, the whole number of peaks and troughs that can be automatically measured by means of DTW is 5,149. The component P600b is not considered because its latency in individual ERPs is often outside the upper boundary of the temporal window used for the alignment. Of these components, 68.56% were correctly identified by the method.

Figure 10 shows the percentage of correct automatic detections for each component. P1 is the potential that was best identified automatically by the method, while the highest number of mistakes was made with N4. In general, the efficacy of the method in the automatic detection of peaks and troughs decreases as latency increases. In fact, the cognitive and

Table 1(a). The latency (ms) of significantly different components ($p < 0.025$) between LPR and LRE in the control group (mean ± standard deviation). Underlined characters indicate $p < 0.01$.

Component		Channel Pz	P4	P3
N1	LPR	101.38 ± 17.75		
	LRE	115.71 ± 17.21		
PmaxB	LPR	308.02 ± 21.86		
	LRE	317.87 ± 20.31		
P600b	LPR		713.30 ± 89.20	693.20 ± 73.77
	LRE		628.72 ± 66.13	624.77 ± 63.80

higher-order components are characterized by a greater latency variability in comparison with those related to lower levels of sensorial processing of stimuli.

Discussion

The analysis of cognitive ERPs recorded in children is difficult because of their marked morphological variability in both amplitude and latency. The necessity of manually measuring the morphological characteristics of these potentials and the inevitable smoothing produced by grand averaging affect the reliability of group analyses. DTW proved to be useful for improving the comparison between the ERPs recorded in different subjects. In fact, it reduces the morphological differences between the signals by stretching and shrinking their temporal axes. The ERP templates of homogeneous groups of subjects had a well-defined and sharper morphology compared to grand averages. Consequently, the quantification of group characteristics (latency and amplitude of the main cerebral components) was more precise and easier to perform.

After the computation of the templates, DTW was used to automatically identify the relevant ERP components by aligning the templates with individual averaged potentials. The method proved to successfully measure a significant percentage of the peaks and troughs present on the traces. The many components contribute differently to the total, because they cannot be clearly identified on all channels and subjects. Taking into account this feature, we computed the percentage of peaks and troughs correctly identified by the method. As could be inferred from the higher latency variability of cognitive components, the efficacy of the method is reduced for long latencies compared to short and middle ones. In order to further improve the method performances, it could be useful to vary the boundaries for computing the WF according to latency, increasing the alignment flexibility for cognitive components.

Combining the automatic identification of ERP components with a manual correction when necessary, we were able to characterize the morphology of reading-related potentials and to extract psychophysiologically relevant differences between normal and dyslexic children. The comparison between the ERPs recorded in normal children during LPR and LRE put into evidence that parietal regions are discriminating for reading aloud versus passive watching of letters. The importance of such areas in reading processes was also pointed out by other studies [17]. Furthermore, the extensive and remarkable increase of amplitude during active reading revealed that the request of an explicit verbal-motor performance activates specific attention processes besides motion-related functions. Considering the group with

Table 1(b). The amplitude (μV) of significantly different components ($p < 0.025$) between LPR and LRE in the control group (mean ± standard deviation). Underlined characters indicate $p < 0.01$.

Component		Channel Fz	Cz	Pz	Oz	C3′	T4	T3	P4	P3
N2	LPR				−9.09 ± 5.87		−6.09 ± 3.00			
	LRE				−11.13 ± 7.11		−7.20 ± 3.23			
PmaxA	LPR	8.07 ± 4.61	9.09 ± 5.80	7.02 ± 6.10		8.43 ± 4.25				
	LRE	10.81 ± 5.78	11.52 ± 6.23	11.24 ± 9.13		10.66 ± 4.94				
PmaxB	LPR				10.21 ± 5.21		5.71 ± 3.69		12.27 ± 7.11	
	LRE				14.93 ± 4.83		7.66 ± 4.56		16.20 ± 7.10	
N3	LPR	−10.86 ± 5.61				−9.77 ± 5.59	−3.71 ± 2.31	−4.39 ± 2.27		
	LRE	−15.08 ± 4.97				−12.02 ± 5.80	−5.20 ± 2.26	−6.87 ± 2.70		
P600a	LPR	3.91 ± 1.93	5.70 ± 3.72	7.16 ± 3.85		4.84 ± 2.58		4.30 ± 2.69	4.22 ± 2.93	5.36 ± 3.22
	LRE	5.97 ± 3.46	9.31 ± 4.63	11.20 ± 5.58		6.98 ± 3.56		5.77 ± 2.71	6.75 ± 3.30	7.82 ± 4.35
P600b	LPR	5.57 ± 2.00						4.87 ± 1.99		
	LRE	10.17 ± 5.47						7.84 ± 4.06		

dyslexia, the comparison between the potentials recorded in the two tasks showed significant latency differences in the frontal and central regions. The amplitude of the potentials in LRE was significantly increased with respect to LPR in almost all the recorded scalp sites, except for the parietal regions. Comparing these observations with those from the control group, it is possible to argue that, when watching letters, the physiological mechanisms that are activated are altered and that the strategies for the organization of reading aloud are abnormal. The direct comparison between the two groups of subjects in each separate task allowed the detection of specific differences in the main ERP components. In the LPR task, the main differences concerned latency, while amplitude differences were negligible. The latency of several ERP components was increased in dyslexic children compared to controls in almost all the EEG channels except for the temporal ones. The latency differences affecting the postlexical components were greater than those affecting the pre- and lexical ones. For the LRE task, the latency of the ERP components in the occipital and temporal regions was increased in dyslexic children compared to controls. The finding of fewer latency differences between the two groups in LRE compared to LPR suggests that the attention processes activated by verbal-motor production contribute to increasing the efficiency of the cerebral reading functions. Significant amplitude differences were found in the central and parietal regions of the left hemisphere, which is undoubtedly involved in language processing.

In conclusion, the method described in this article improves the comparison of ERPs recorded in different groups of subjects—and in different experimental conditions—through the computation of proper templates representing the relevant group of cerebral potentials without morphological alterations. Furthermore, the partially automatic identification of features allowed by the method makes the analysis of ERPs easier, quicker, and more reliable because the subjective manual intervention of the experimenter is reduced. The comparison between the potentials recorded in normal children during two reading conditions, which were characterized by increasing cognitive effort, highlighted some physiological strategies activated during reading.

In particular, reading aloud likely activates attention processes that are able to recruit larger neuronal resources for the execution of the task. The visual presentation of single letters employed in this experimental setting led the cerebral activity focusing on the strict association between graphemes and phonemes. In this condition, we evaluated the poor efficiency of dyslexic children in building and employing a cerebral map of correspondence between written letters and their sounds. The most evident difference between the two groups of subjects in both reading tasks is an extensive delay of the main ERP components. This delay increases from shorter to longer latencies. The involvement of several components related to perceptive functions, memory, attention, and cognitive processes shows that dyslexia is a pathology in which not only the reading mechanisms, but also more general functions, at different time scales are compromised. The finding of group differences in the right hemisphere supports the hypothesis of dyslexia as a spread disorder which is not limited to the classical brain areas normally involved in linguistic abilities.

The use of mathematical procedures for quantifying ERPs' morphology is critical for making the analysis of cognitive potentials independent from the subjective judgment of the experimenter. Furthermore, the comparison among studies realized by different research laboratories would benefit from the implementation of more reproducible analysis criteria.

Table 2(a). The latency (ms) of significantly different components ($p < 0.025$) between LPR and LRE in children with dyslexia (mean ± standard deviation). Underlined characters indicate $p < 0.01$.

		Channel			
Component		Fz	Cz	Oz	P3
N1	LPR	129.56 ± 17.95	129.93 ± 21.78		
	LRE	113.46 ± 17.05	106.41 ± 16.90		
N3	LPR			425.20 ± 29.10	406.61 ± 26.18
	LRE			394.96 ± 24.95	383.17 ± 24.61

Table 2(b). The amplitude (μV) of significantly different components ($p < 0.025$) between LPR and LRE in children with dyslexia (mean ± standard deviation). Underlined characters indicate $p < 0.01$.

		Channel						
Component		Fz	Cz	Pz	Oz	C4′	T4	T3
N1	LPR						−1.64 ± 1.30	−2.75 ± 1.28
	LRE						−3.24 ± 1.38	−3.32 ± 1.30
PmaxA	LPR		9.73 ± 3.31					
	LRE		13.01 ± 4.61					
PmaxB	LPR				9.67 ± 6.11			
	LRE				14.30 ± 7.37			
N3	LPR		−9.20 ± 4.07					
	LRE		−13.26 ± 6.83					
P600a	LPR		5.62 ± 4.21	6.83 ± 5.08		3.72 ± 1.89		
	LRE		10.39 ± 4.45	12.35 ± 6.35		6.87 ± 2.18		
P600b	LPR	5.29 ± 1.59						
	LRE	9.30 ± 4.09						

Table 3(a). The latency (ms) of significantly different components ($p < 0.025$) between normal children (N) and children with dyslexia (D) during LPR (mean ± standard deviation). Underlined characters indicate $p < 0.01$.

Component		Channel							
		Fz	Cz	Pz	Oz	C4′	C3′	P4	P3
P0	N			80.72 ± 18.63					
	D			103.42 ± 20.05					
N1	N	114.37 ± 17.94	110.54 ± 15.76			110.73 ± 13.14	113.01 ± 16.33		
	D	130.59 ± 19.07	131.37 ± 22.07			124.42 ± 18.61	128.98 ± 17.86		
PmaxA	N			224.97 ± 22.51				232.21 ± 21.08	226.56 ± 19.42
	D			251.23 ± 29.26				257.34 ± 17.66	265.29 ± 16.79
N3	N			387.97 ± 19.24	392.33 ± 26.52				
	D			405.61 ± 26.78	421.11 ± 27.64				
P600a	N				453.08 ± 35.53			457.45 ± 39.75	
	D				489.49 ± 29.24			495.51 ± 31.91	

Table 3(b). The amplitude (μV) of significantly different components ($p < 0.025$) between normal children (N) and children with dyslexia (D) during LPR (mean ± standard deviation). Underlined characters indicate $p < 0.01$.

Component		Channel
		Cz
N2	N	−2.39 ± 1.20
	D	−4.71 ± 2.71

Table 4(a). The latency (ms) of significantly different components ($p < 0.025$) between normal children (N) and children with dyslexia (D) during LRE (mean ± standard deviation). Underlined characters indicate $p < 0.01$.

Component		Channel		
		Oz	T4	T3
N1	N		107.26 ± 10.52	109.22 ± 13.14
	D		120.79 ± 19.02	121.90 ± 19.75
P1	N		143.06 ± 13.27	
	D		152.88 ± 13.26	
N2	N			180.85 ± 14.30
D				199.40 ± 22.14
PmaxA	N	211.19 ± 23.47		
	D	240.00 ± 23.76		
P600a	N	457.41 ± 32.65		
	D	496.19 ± 31.24		

Table 4(b). The amplitude (μV) of significantly different components ($p < 0.025$) between normal children (N) and children with dyslexia (D) during LRE (mean ± standard deviation). Underlined characters indicate $p < 0.01$.

Component		Channel	
		C3′	P3
N2	N	−2.68 ± 2.05	
	D	−4.59 ± 1.73	
N3	N		−9.64 ± 5.34
	D		−6.17 ± 3.26

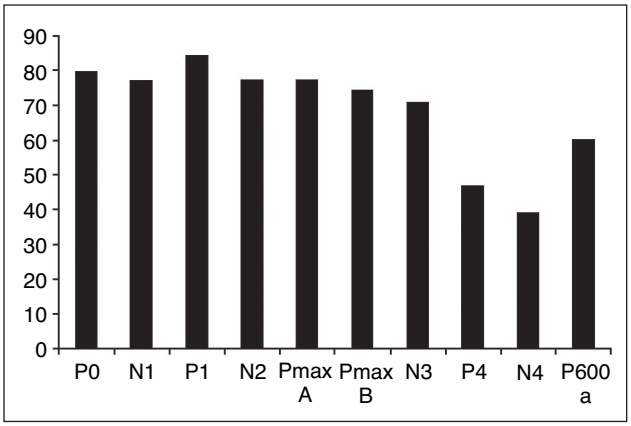

Fig. 10. The percentage of correct automatic detections for each component.

Silvia Casarotto graduated with an M.A. in biomedical engineering, with an emphasis in neural signals processing, from the Polytechnic University of Milan, Italy, in 2002. She is currently a Ph.D. student of bioengineering at the same university. Her current research focuses on the integration of electrophysiology and functional neuroimaging for investigating the reading processes in normal children and in children affected by developmental dyslexia.

Anna M. Bianchi received the Laurea degree in electronic engineering from the Polytechnic University of Milan, Italy, in 1987. Afterwards, she was a research fellow in the Laboratory of Biomedical Engineering at San Raffaele Hospital in Milan, Italy, and from 1990 to 2000 she was a research assistant in the same laboratory. Now, she is a researcher at the Department of Biomedical Engineering of the Polytechnic University of Milan, and she is also a professor of electronic bioengineering foundations in the biomedical engineering course at the university. Her research interests are mainly related to biomedical signal processing and biomedical system modeling, with particular applications to the cardiovascular and neurosensorial systems. She is studying and developing methods and algorithms for time-frequency analysis of nonstationary signals, including time frequency distributions, wavelets, and recursive parametric identification. She is the published author of various papers and book chapters on these topics.

Sergio Cerutti received the Laurea degree in electronic engineering from the Polytechnic University of Milan, Italy, in 1971. From 1982 to 1990 he was an associate professor of biomedical engineering at the Department of Electrical Engineering and, later, at the Department of Biomedical Engineering of the same university. He has been a professor of biomedical signal and data processing for the Department of Biomedical Engineering since 1994 and the department's director since 2000. From 1990 to 1994, he was a professor of biomedical engineering at the Department of Computer and System Sciences of the University of Rome "La Sapienza," Italy.

His research activity is mainly dedicated to various aspects of biomedical signal and data processing and modeling related to the cardiovascular system and in the field of neurosciences. He is the author of more than 250 papers on these topics published in qualified international scientific literature. He has coordinated various research projects at national and international levels in various topics of biomedical engineering and bioinfomatics. He spent over a year as a visiting professor at the Massachusetts Institute of Technology and the Harvard School of Public Health, Boston, Massachusetts. He has been chairman of the bachelor track in biomedical engineering of the same polytechnic from 1996–2000. He is chairman of the Biomedical Engineering Group of the Italian AEI (Association of Electrical Engineering). He is a member of IEEE-AEI, IFMBE-AIIMB, ESEM, IEC-CEI and other international and national scientific associations. He is on the editorial board of various biomedical engineering journals; in particular, he is an associate editor of IEEE Transactions on Biomedical Engineering. He also has been the organizer of three IEEE-EMBS International Summer Schools on Biomedical Signal Processing held in Siena, Italy. He was also elected member of the Consultive Committee 09-Industrial Engineering of CUN (University National Committee) from 1988–1996 and was secretary of the same consultive committee.

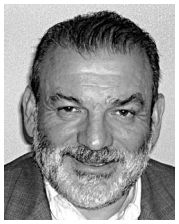

Giuseppe A. Chiarenza received medical postgraduate training in child and adolescent neuropsychiatry and neurology. He has been a senior researcher at Milan University. He is currently head of the Mental Health Department of Azienda Ospedaliera "G. Salvini," Garbagnate Milanese (Milan, Italy) and director of the Child and Adolescent Neuropsychiatry Unit of Rho Hospital. He is also a professor of child neuropsychiatry at the Catholic University of Piacenza. He is actively working in the developmental neuropsychology field, with particular interest on dyslexia and attention deficit hyperactivity disorder.

Address for Correspondence: Silvia Casarotto, via Buozzi 11, 20085 Locate Triulzi, Milan, Italy. Phone: +39 02 90730850, +39 338 4897257. Fax: +39 02 90730850. E-mail: silvia.casarotto@polimi.it.

References

[1] W.E. Brown, S. Eliez, V. Menon, C.D. White, and A.L. Reiss, "Preliminary evidence of widespread morphological variations of the brain in dyslexia," *Neurology*, vol. 56, no. 6, pp. 781–783, 2001.

[2] M. Habib, "The neurological basis of developmental dyslexia," *Brain*, vol. 123, pp. 2373–2399, 2000.

[3] F. Ramus, "Talk of two theories," *Nature*, vol. 412, no. 6845, pp. 393–395, 2001.

[4] S.E. Shaywitz, B.A. Shaywitz, K.R. Pugh, R.K. Fulbright, R.T. Constable, W.E. Mencl, D.P. Shankweiler, A.M. Liberman, P. Skudlarski, J.M. Fletcher, L. Katz, K.E. Marchine, C. Lacadie, C. Gatenby, and J.C. Gore, "Functional disruption in the organization of the brain for reading in dyslexia," *Proc. Natl. Acad. Sci. USA*, vol. 95, no. 5, pp. 2636–2641, 1998.

[5] E.L. Grigorenko, "Developmental dyslexia: An update on genes, brains and environments," *J. Child Psychol. Psychiat.*, vol. 42, no. 1, pp. 91–125, 2001.

[6] E. Paulesu, J-F. Dèmonet, F. Fazio, E. McCrory, V. Chanoine, N. Brunswick, S.F. Cappa, G. Cossu, M. Habib, C.D. Frith, and U. Frith, "Dyslexia: Cultural diversity and biological unity," *Science*, vol. 291, no. 5511, pp. 2165–2167, 2001.

[7] G.A. Chiarenza, "Linee guida dei disturbi specifici di apprendimento," *Giornale Italiano di Neuropsichiatria Infantile*, vol. 24, pp. 79–95, 2004.

[8] J. Intriligator and J. Polich, "On the relationship between EEG and ERP variability," *Int. J. Psychophysiology*, vol. 20, no. 1,pp. 59–74, 1995.

[9] E.G. Caiani, A. Porta, G. Baselli, M. Turiel, S. Muzzupappa, M. Pagani, A. Malliani, and S. Cerutti, "Analysis of cardiac left-ventricular volume based on time warping averaging," *Med. Biol. Eng. Comput.*, vol. 40, no. 2, pp. 225–233, 2002.

[10] H. Sakoe and S. Chiba, "Dynamic programming algorithm optimisation for spoken word recognition," *IEEE Trans. Acoust., Speech, Signal Processing*, vol. 26, no. 1, pp. 43–49, Feb. 1978.

[11] American Psychiatric Association, *Diagnostic and statistical manual of mental disorders*, 4th ed. Washington, DC: American Psychiatric Association, 1994.

[12] E. Boder, "Developmental dyslexia: A diagnostic approach based on 3 atypical reading-spelling patterns," *Dev. Med. Child Neurol.*, vol. 15, no. 5, pp. 663–687, 1973.

[13] G.A. Chiarenza and D. Bindelli, "Il test diretto di lettura e scrittura (TDLS): Versione computerizzata e dati normativi," *Giornale di Neuropsichiatria dell'eta` Evolutiva*, vol. 21, no. 2, pp. 163–179, 2001.

[14] S. Casarotto, A.M. Bianchi, S. Cerutti, and G.A. Chiarenza, "Principal component analysis for reduction of ocular artefacts in event-related potentials of normal and dyslexic children," *Clinical Neurophysiology*, vol. 115, no. 3, pp. 609–619, 2004.

[15] E. Courchesne, "Neurophysiological correlates of cognitive development: Changes in long-latency event-related potentials from childhood to adoulthood," *Electr. Clin. Neurophysiol.*, vol. 45, no. 4, pp. 468–482, 1978.

[16] R. Licht, D.J. Bakker, A. Kok, and A. Bouma, "The development of lateral event-related potentials (ERPs) related to word naming: A four year longitudinal study," *Neuropsychologia*, vol. 26, no. 2, pp. 327–340, 1988.

[17] J.A. Fiez and S.E. Petersen, "Neuroimaging studies of word reading," *Proc. Natl. Acad. Sci. USA*, vol. 95, no. 3, pp. 914–921, 1998.